Evaluation of Variable Kinematics Beam, Plate, and Shell Theories using the Asymptotic-Axiomatic Method

E. Carrera[1], D. Scano[2], M. Petrolo[3]

MUL[2] Lab, Department of Mechanical and Aerospace Engineering,
Politecnico di Torino, Corso Duca degli Abruzzi 24, 10129 Torino, Italy

Revised version of MechSol2460643Carrera

Author for correspondence:
Marco Petrolo
MUL[2] Lab, Department of Mechanical and Aerospace Engineering,
Politecnico di Torino,
Corso Duca degli Abruzzi 24,
10129 Torino, Italy,
tel: +39 011 090 6845,
e-mail: marco.petrolo@polito.it

[1] Professor of Aeronautics and Astronautics. E-mail: erasmo.carrera@polito.it
[2] PhD Student. E-mail: daniele.scano@polito.it
[3] Associate Professor. E-mail: marco.petrolo@polito.it

Evaluation of Variable Kinematics Beam, Plate, and Shell Theories using the Asymptotic-Axiomatic Method

E. Carrera[a,*] and D. Scano[a,] and M. Petrolo[a,***]**

[a]MUL2 Lab, Department of Mechanical and Aerospace Engineering,

Politecnico di Torino, Corso Duca degli Abruzzi 24, 10129 Torino, Italy

[*]e-mail: erasmo.carrera@polito.it, [**]e-mail: daniele.scano@polito.it,

[***]e-mail: marco.petrolo@polito.it,

Received xx.xx.xxxx;

revised xx.xx.xxxx;

accepted xx.xx.xxxx.

Abstract –This paper proposes a novel approach to evaluate structural theories based on their accuracy and computational efficiency. The focus is on beam, plate, and shell theories built using polynomial expansions of the displacement field. The structural theories and related finite element matrices are obtained through the Carrera Unified Formulation. Each displacement component can have different expansions, and the choice of the generalized variables to include is an input for the analysis. Similar results were obtained in previous works through penalization techniques applied to the finite element matrices. This paper presents a novel approach to building finite element matrices based on truncated expansions of the unknown variables, leading to smaller matrices and lower computational costs. Best theories concerning accuracy and computational costs are retrieved and presented through Best Theory Diagrams. Numerical results consider verification with data from literature and the analysis of structural problems with localized effects, such as pinched shell and end-effect problems. The results show the importance of correctly choosing the generalized variables, which may lead to reduced computational costs with negligible accuracy loss.

Keywords: Finite element method; beams, plates and shells; Carrera Unified Formulation; Asymptotic-Axiomatic Method.

1. INTRODUCTION

The development of beam and plate/shell theories is a classical topic in structural engineering. There is a preference for one-dimensional (1D) and two-dimensional (2D) models over more complex three-dimensional (3D) analyses. Despite advancements in computational mechanics and computing power, beam and plate/shell models remain popular due to their computational efficiency.

Beams find extensive applications in engineering, ranging from aircraft wings and helicopter rotor blades in aerospace engineering to civil engineering structures composed of metallic and concrete beams. Plates and shells are equally important, e.g., for aircraft panels and cylindrical

structures in the aerospace field. Beam and plate/shell models can be categorized into two types: axiomatic models, which assume the structural behavior, and asymptotic models, which derive beam or plate/shell expansions of the governing equations considering characteristic parameters, e.g., the thickness ratio.

The Euler-Bernoulli [1] beam theory (EBBT) is often used to analyze isotropic slender structures; however, it does not account for shear effects. The Timoshenko [2] beam theory (TBT) extends EBBT, including shear effects. Many scholars have proposed more advanced beam theories to overcome EBBT and TBT limitations [3, 4]. Washizu [5] underlined the need for higher-order theories and proposed a general expansion with N terms for the three displacement variables based on polynomial terms:

$$\begin{aligned} u_x &= u_{x_1} + xu_{x_2} + zu_{x_3} + x^2u_{x_4} + xzu_{x_5} + z^2u_{x_6} + \cdots + x^a z^b u_{x_N} \\ u_y &= u_{y_1} + xu_{y_2} + zu_{y_3} + x^2u_{y_4} + xzu_{y_5} + z^2u_{y_6} + \cdots + x^a z^b u_{y_N} \\ u_z &= u_{z_1} + xu_{z_2} + zu_{z_3} + x^2u_{z_4} + xzu_{y_5} + z^2u_{z_6} + \cdots + x^a z^b u_{z_N} \end{aligned} \tag{1.1}$$

The torsion of thin-walled beams has known many contributions, starting from Vlasov [6], who introduced warping functions. Other examples of works on warping functions are those by Friberg [7] and Mechab *et al.* [8]. Schardt [9] introduced the Generalized Beam Theory, which enhances classical theories by using piece-wise kinematics of thin-walled sections to detect warping and distortions. Ganapathi *et al.* [10] developed a three-node finite element (FE) that includes transverse shear and torsion with warping. Levinson [11] proposed a theory incorporating warping while respecting shear-free conditions on the lateral surfaces. Wang and Li [12] adopted the Levinson beam theory in free vibration problems. Kant and Manjunath [13, 14, 15] studied laminated composite beams by using higher-order models in the context of C^0 FE with first to fourth-order models. Kapania and Goyal [16] proposed a two-node FE to study laminated beams with uncertainties in the ply orientations. Bui *et al.* [17] studied thin-walled composite structures with I-sections using higher-order terms for all three displacement components. Carrera introduced the Unified Formulation (CUF) for beams [18] where the cross-section kinematics may be modeled using various types of functions, e.g., Taylor expansions [19] or Lagrange [20].

Many plate and shell theories have been proposed over the years [21]. The Thin Plate Theory (TPT) and Thin Shell Theory (TST) are the classical models based on Kirchhoff's hypotheses [22]; they neglect the transverse shear deformation and the through-the-thickness deformation.

A refinement, including the transverse shear deformation, is the Reissner–Mindlin theory [23, 24], which is also known as the First-Order Shear Deformation Theory (FSDT). More advanced plate/shell theories have been used to study thick and laminated structures [25, 26, 27, 28, 29, 30]. Grigolyuk *et al.* [31, 32] presented excellent reviews on the principal contributions of the Soviet

scientific community. Kant *et al.* [33] developed a nine-node Lagrange plate element with six degrees of freedom (DOF) per node. Kant and Majunatha [34] introduced third-order plate theory for all displacement components, while in Pandya and Kant [35], the transverse displacement was kept constant. Sheremetev and Pelekh [36], and later on, Whitney, Pagano [37], and Reddy [38] proposed models to fulfill the top and bottom boundary conditions. Reddy and Liu [39] developed refined shell models to account for the parabolic distribution of transverse shear stresses in static and dynamic analyses. Awrejcewicz *et al.* [40] made an historical dissertation on who first proposed these types of theories for two-dimensional structures. Bhiramaddi [41] considered circular cylindrical shells by including higher-order terms for in-plane displacements, whereas the stretching of the structure was not considered. Other researchers have proposed models with parabolic approximations of the transverse displacement component, e.g., Hildebrand *et al.* [42] and Khare *et al.* [43]. CUF was also developed for plate and shell formulations [44] Taylor, Lagrange, and Legendre expansions over the thickness have been adopted [45, 46, 47].

As mentioned, the axiomatic approach employs variationally consistent governing equations, achieving asymptotically exact results. Volovoi *et al.* [48] investigated open cross-section and thin-walled structures by applying the variational-asymptotic method, using 3D models as reference results. Volovoi and Hodges [49] extended this method to beams with arbitrary cross sections. Popescu and Hodges [50] considered shear deformations. Yu *et al.* [51] introduced the Variational Asymptotic Beam Sectional Analysis (VABS) to address anisotropic beams, including initially curved and twisted beams. Asymptotic models have also been developed for plates and shells [52, 53, 54]. Lee and Hodges [55] used FEM for the dynamic analysis of shells. Berdichevsky [56] investigated sandwich shells.

This work aims to develop a method for evaluating the impact of each generalized variable of higher-order beam, plate, and shell theories and based on the Asymptotic-Axiomatic Method (AAM) proposed by Carrera and collaborators for [57, 58]. The best theories are obtained by retaining only those variables having a significant role in the solution, offering the highest accuracy possible with a given amount of DOF. all theories and their optimal distributions for free vibrations. In previous works, a penalization technique was used to assess best theories. This paper, instead, presents a new approach to building finite element matrices in which each displacement variable can be analyzed using a distinct expansion function node-wise, enabling the selection of various polynomial-based theories within a unified framework.

This paper is organized as follows: Section 2 provides an overview of beam, plate and shell theories; Section 3 introduces CUF and the related FEM formulation; Section 4 presents the

governing equations; Section 5 concerns the AAM and the obtaining of related FE matrices; Section 6 presents and discusses the results, and conclusions are in Section 7.

2. CLASSICAL AND ADVANCED BEAM, PLATE AND SHELL THEORIES

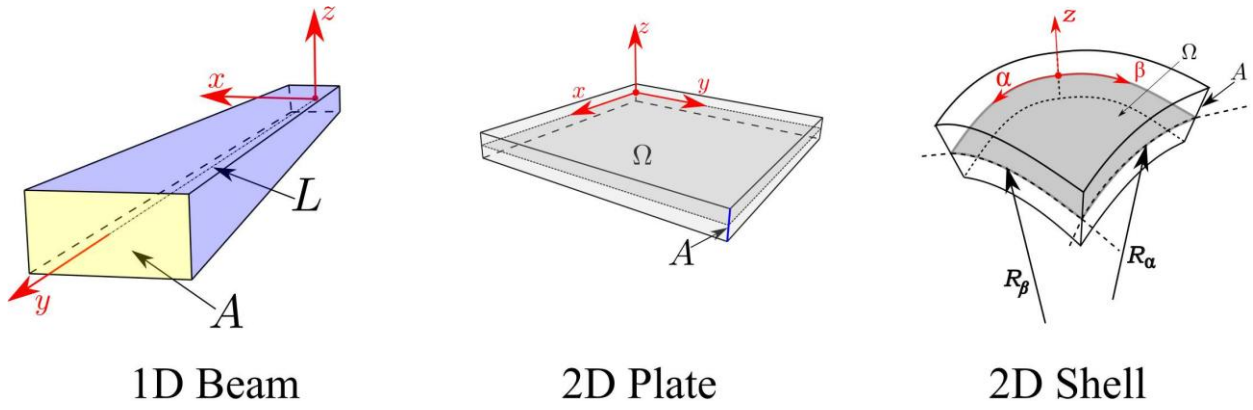

Fig. 1. Reference systems for 1D and 2D structures

Let us consider the isotropic beam, plate, and shell structures in Fig. 1. A Cartesian reference system is adopted for the beam and the plate. The beam's cross-section, A, lies in the x-z plane, while the beam axis, denoted as L, is aligned with the y-direction. In plates, the thickness line A lays along the z-direction. A curvilinear reference system is considered in the shell case. The mid-surface is denoted by **Ω** and the thickness-line *A* lays along the z-direction. The shell has two radii of curvature, namely, R_α and R_β. A plate may be seen as a shell with infinite radii. For brevity, only the shell formulation is described in this paper.

The three-dimensional displacement fields are given by the following vectors:

BEAM: $$\mathbf{u}(x,y,z) = \{u_x(x,y,z), u_y(x,y,z), u_z(x,y,z)\}^T \tag{2.1}$$

SHELL: $$\mathbf{u}(\alpha,\beta,z) = \{u_\alpha(\alpha,\beta,z), u_\beta(\alpha,\beta,z), u_z(\alpha,\beta,z)\}^T \tag{2.2}$$

2.1. Classical beam theories

A beam is referred to a bar or a rod [59] if only the constant terms of the displacement field are considered,

$$\begin{aligned} u_x(x,y,z) &= u_{x_1}(y) \\ u_y(x,y,z) &= u_{y_1}(y) \\ u_z(x,y,z) &= u_{z_1}(y) \end{aligned} \tag{2.3}$$

One of the most known displacement-based theory is the Euler-Bernoulli [1] Beam Theory (EBBT),

$$\begin{aligned} u_x(x,y,z) &= u_{x_1}(y) \\ u_y(x,y,z) &= u_{y_1}(y) - \frac{\partial u_{x_1}(y)}{\partial y} - \frac{\partial u_{z_1}(y)}{\partial y} \\ u_z(x,y,z) &= u_{z_1}(y) \end{aligned} \tag{2.4}$$

On the other hand, the displacement field of the Timoshenko [2] Beam Theory (TBT) reads:

$$\begin{aligned} u_x(x,y,z) &= u_{x_1}(y) \\ u_y(x,y,z) &= u_{y_1}(y) + \phi_z(y)x + \phi_x(y)z \\ u_z(x,y,z) &= u_{z_1}(y) \end{aligned} \tag{2.5}$$

ϕ_z and ϕ_x are the rotations around the z and x axes, respectively. The simplest beam model including torsion [5] is

$$\begin{aligned} u_x(x,y,z) &= z\theta(y) \\ u_y(x,y,z) &= 0 \\ u_z(x,y,z) &= -x\theta(y) \end{aligned} \tag{2.6}$$

θ is the rigid rotation of the cross-section about the y-axis.

2.2. Classical plate/shell theories

The displacement field of the membrane theory [59] reads:

$$\begin{aligned} u_\alpha(\alpha,\beta,z) &= u_{\beta_1}(\alpha,\beta) \\ u_\beta(\alpha,\beta,z) &= u_{\alpha_1}(\alpha,\beta) \\ u_z(\alpha,\beta,z) &= u_{z_1}(\alpha,\beta) \end{aligned} \tag{2.7}$$

The Thin Shell Theory (TST) [22] has the following displacement:

$$\begin{aligned} u_\alpha(\alpha,\beta,z) &= u_{\alpha_1}(\alpha,\beta) - \frac{\partial u_{z_1}(\alpha,\beta)}{\partial \alpha} z \\ u_\beta(\alpha,\beta,z) &= u_{\beta_1}(\alpha,\beta) - \frac{\partial u_{z_1}(\alpha,\beta)}{\partial \beta} z \\ u_z(\alpha,\beta,z) &= u_{z_1}(\alpha,\beta) \end{aligned} \tag{2.8}$$

On the other hand, the First-order Shear Deformation Theory (FSDT) [23, 24] is

$$\begin{aligned} u_\alpha(\alpha,\beta,z) &= u_{\alpha_1}(\alpha,\beta) - \frac{\partial u_{z_1}(\alpha,\beta)}{\partial \alpha} z \\ u_y(\alpha,\beta,z) &= u_{\beta_1}(\alpha,\beta) - \frac{\partial u_{z_1}(\alpha,\beta)}{\partial \beta} z \\ u_z(\alpha,\beta,z) &= u_{z_1}(\alpha,\beta) \end{aligned} \tag{2.9}$$

ϕ_β and ϕ_α are the rotations around the β and α axes, respectively.

2.3. Examples of higher-order theories

Adding terms to the displacement field is one way to build higher-order theories. For brevity, a couple of examples for 2D models are presented here, as similar expansions can also be used for 1D cases. One of the earliest models was introduced by Hildebrand, Reissner, and Thomas (HRT) [42], where the u_z includes first and second-order terms,

$$
\begin{aligned}
u_\alpha(\alpha,\beta,z) &= u_{\alpha_1}(\alpha,\beta) + z u_{\alpha_2}(\alpha,\beta) \\
u_y(\alpha,\beta,z) &= u_{\beta_1}(\alpha,\beta) + z u_{\beta_2}(\alpha,\beta) \\
u_z(\alpha,\beta,z) &= u_{z_1}(\alpha,\beta) + z u_{z_2}(\alpha,\beta) + z^2 u_{z_3}(\alpha,\beta)
\end{aligned}
\tag{2.10}
$$

Khare *et al.* [43], instead, extended the model of Sheremetev and Pelekh [36] for composite shells,

$$
\begin{aligned}
u_\alpha(\alpha,\beta,z) &= u_{\alpha_1}(\alpha,\beta) + z u_{\alpha_2}(\alpha,\beta) + z^2 u_{\alpha_3}(\alpha,\beta) + z^3 u_{\alpha_4}(\alpha,\beta) \\
u_\beta(\alpha,\beta,z) &= u_{\beta_1}(\alpha,\beta) + z u_{\beta_2}(\alpha,\beta) + z^2 u_{\beta_3}(\alpha,\beta) + z^3 u_{\beta_4}(\alpha,\beta) \\
u_z(\alpha,\beta,z) &= u_{z_1}(\alpha,\beta) + z u_{z_2}(\alpha,\beta) + z^2 u_{z_3}(\alpha,\beta)
\end{aligned}
\tag{2.11}
$$

2.4. Taylor-based higher-order theories

The present paper adopts Taylor polynomials to build higher-order theories. Complete and reduced expansions are used, and this section provides some examples. A complete expansion adopts the same terms for the three displacement variables. A second-order beam theory (TE2) can be expressed as follows:

$$
\begin{aligned}
u_x(x,y,z) &= u_{x_1}(y) + x u_{x_2}(y) + z u_{x_3}(y) + x^2 u_{x_4}(y) + xz u_{x_5}(y) + z^2 u_{x_6}(y) \\
u_y(x,y,z) &= u_{y_1}(y) + x u_{y_2}(y) + z u_{y_3}(y) + x^2 u_{y_4}(y) + xz u_{y_5}(y) + z^2 u_{y_6}(y) \\
u_z(x,y,z) &= u_{z_1}(y) + x u_{z_2}(y) + z u_{z_3}(y) + x^2 u_{z_4}(y) + xz u_{y_5}(y) + z^2 u_{z_6}(y)
\end{aligned}
\tag{2.12}
$$

In a FEM scenario, such a beam model has 18 nodal degrees of freedom (DOF). Similarly, a fifth-order shell model (TE5) is

$$
\begin{aligned}
u_\alpha(\alpha,\beta,z) &= u_{\alpha_1}(\alpha,\beta) + z u_{\alpha_2}(\alpha,\beta) + z^2 u_{\alpha_3}(\alpha,\beta) + z^3 u_{\alpha_4}(\alpha,\beta) + z^4 u_{\alpha_5}(\alpha,\beta) + z^5 u_{\alpha_6}(\alpha,\beta) \\
u_y(\alpha,\beta,z) &= u_{\beta_1}(\alpha,\beta) + z u_{\beta_2}(\alpha,\beta) + z^2 u_{\beta_3}(\alpha,\beta) + z^3 u_{\beta_4}(\alpha,\beta) + z^4 u_{\beta_5}(\alpha,\beta) + z^5 u_{\beta_6}(\alpha,\beta) \\
u_z(\alpha,\beta,z) &= u_{z_1}(\alpha,\beta) + z u_{z_2}(\alpha,\beta) + z^2 u_{z_3}(\alpha,\beta) + z^3 u_{z_4}(\alpha,\beta) + z^4 u_{z_5}(\alpha,\beta) + z^5 u_{z_6}(\alpha,\beta)
\end{aligned}
\tag{2.13}
$$

Reduced expansions, on the other end, use only some terms of the expansion, and these terms may differ for each displacement component, e.g.,

BEAM:

$$
\begin{aligned}
u_x(x,y,z) &= u_{x_1}(y) + z u_{x_2}(y) \\
u_y(x,y,z) &= u_{y_1}(y) + x u_{y_2}(y) + xz u_{y_3}(y) + z^2 u_{y_4}(y) \\
u_z(x,y,z) &= u_{z_1}(y)
\end{aligned}
\tag{2.14}
$$

SHELL:

$$
\begin{aligned}
u_\alpha(\alpha,\beta,z) &= u_{\alpha_1}(\alpha,\beta) + z^2 u_{\alpha_2}(\alpha,\beta) \\
u_\beta(\alpha,\beta,z) &= u_{\beta_1}(\alpha,\beta) + z u_{\beta_2}(\alpha,\beta) + z^3 u_{\beta_3}(\alpha,\beta) + z^5 u_{\beta_4}(\alpha,\beta) \\
u_z(\alpha,\beta,z) &= u_{z_1}(\alpha,\beta)
\end{aligned}
\tag{2.15}
$$

3. UNIFIED FORMULATION OF ANY-ORDER THEORIES

The present paper uses the Carrera Unified Formulation (CUF) to obtain the displacement field, governing equations, and FE matrices of structural theories of any order.

In the CUF, to reduce a 3D problem into a 1D or a 2D one, a primary variable (f), such as displacement, stress, or strain components, is given by expansion functions having "M" terms (f_τ, τ=1,..., M). In a beam formulation, the expansion uses 2D functions, $F_\tau(x,z)$, defined over the beam cross-section. On the contrary, in 2D formulations, $F_\tau(z)$ are defined through the thickness, i.e.,

BEAM: $$f(x,y,z) = F_\tau(x,z) f_\tau(y) \qquad \tau = 1, \dots, M \tag{3.1}$$

SHELL: $$f(\alpha,\beta,z) = F_\tau(z) f_\tau(\alpha,\beta) \qquad \tau = 1, \dots, M \tag{3.2}$$

The Einstein's summation rule is used. The displacement field, then, becomes

BEAM: $$\begin{aligned} u_x(x,y,z) &= F_{u_x\tau}(x,z) u_{x_\tau}(y) \text{ with } \tau = 1, \dots, M_{u_x} \\ u_y(x,y,z) &= F_{u_y\tau}(x,z) u_{y_\tau}(y) \text{ with } \tau = 1, \dots, M_{u_y} \\ u_z(x,y,z) &= F_{u_z\tau}(x,z) u_{z_\tau}(y) \text{ with } \tau = 1, \dots, M_{u_z} \end{aligned} \tag{3.3}$$

SHELL: $$\begin{aligned} u_x(\alpha,\beta,z) &= F_{u_\alpha\tau}(z) u_{\alpha_\tau}(\alpha,\beta) \text{ with } \tau = 1, \dots, M_{u_\alpha} \\ u_y(\alpha,\beta,z) &= F_{u_\beta\tau}(z) u_{\beta_\tau}(\alpha,\beta) \text{ with } \tau = 1, \dots, M_{u_\beta} \\ u_z(\alpha,\beta,z) &= F_{u_z\tau}(z) u_{z_\tau}(\alpha,\beta) \text{ with } \tau = 1, \dots, M_{u_z} \end{aligned} \tag{3.4}$$

M_{ux}, M_{uy}, and M_{uz} indicate the number of expansion terms for each displacement component. CUF may be combined with FEM to discretize the displacements along the beam axis or over the plate/shell mid-surface. Thus, the displacements can be expressed as follows:

BEAM: $$\begin{aligned} u_x(x,y,z) &= N_i(y) F_{u_x\tau}(x,z) q_{x_{\tau i}} \text{ with } \tau = 1, \dots, M_{u_x} \text{ and } i = 1, \dots, N_n \\ u_y(x,y,z) &= N_i(y) F_{u_y\tau}(x,z) q_{y_{\tau i}} \text{ with } \tau = 1, \dots, M_{u_y} \text{ and } i = 1, \dots, N_n \\ u_z(x,y,z) &= N_i(y) F_{u_z\tau}(x,z) q_{z_{\tau i}} \text{ with } \tau = 1, \dots, M_{u_z} \text{ and } i = 1, \dots, N_n \end{aligned} \tag{3.5}$$

SHELL: $$\begin{aligned} u_\alpha(\alpha,\beta,z) &= N_i(\alpha,\beta) F_{u_\alpha\tau}(z) q_{\alpha_{\tau i}} \text{ with } \tau = 1, \dots, M_{u_\alpha} \text{ and } i = 1, \dots, N_n \\ u_\beta(\alpha,\beta,z) &= N_i(\alpha,\beta) F_{u_\beta\tau}(z) q_{\beta_{\tau i}} \text{ with } \tau = 1, \dots, M_{u_\beta} \text{ and } i = 1, \dots, N_n \\ u_z(\alpha,\beta,z) &= N_i(\alpha,\beta) F_{u_z\tau}(z) q_{z_{\tau i}} \text{ with } \tau = 1, \dots, M_{u_z} \text{ and } i = 1, \dots, N_n \end{aligned} \tag{3.6}$$

N_i and N_j are the shape functions, the repeated subscripts i and j indicate summation, and N_n is the number of nodes per element. This work employs four-node Lagrange beam (B4) and nine-node Lagrange shell (Q9) elements for the beam and plate/shell formulations, respectively.

4. GOVERNING EQUATIONS AND FINITE ELEMENTS

The stress and strain components are grouped as follows:

$$\boldsymbol{\sigma} = \{\sigma_{xx} \quad \sigma_{yy} \quad \sigma_{zz} \quad \sigma_{xz} \quad \sigma_{yz} \quad \sigma_{xy}\}^T \qquad \boldsymbol{\epsilon} = \{\epsilon_{xx} \quad \epsilon_{yy} \quad \epsilon_{zz} \quad \epsilon_{xz} \quad \epsilon_{yz} \quad \epsilon_{xy}\}^T \tag{4.1}$$

$$\boldsymbol{\sigma} = \{\sigma_{\alpha\alpha} \quad \sigma_{\beta\beta} \quad \sigma_{zz} \quad \sigma_{\alpha z} \quad \sigma_{\beta z} \quad \sigma_{\alpha\beta}\}^T \quad \boldsymbol{\epsilon} = \{\epsilon_{\alpha\alpha} \quad \epsilon_{\beta\beta} \quad \epsilon_{zz} \quad \epsilon_{\alpha z} \quad \epsilon_{\beta z} \quad \epsilon_{\alpha\beta}\}^T \tag{4.2}$$

The geometric relationships between strains and displacements can be defined as

$$\boldsymbol{\epsilon} = \mathbf{D}\boldsymbol{u} \tag{4.3}$$

D is a matrix of differential operators; in the linear case,

$$\mathbf{D}_{\text{BEAM}} = \begin{bmatrix} \partial_x & 0 & 0 \\ 0 & \partial_y & 0 \\ 0 & 0 & \partial_z \\ \partial_z & 0 & \partial_x \\ 0 & \partial_z & \partial_y \\ \partial_y & \partial_x & 0 \end{bmatrix} \quad \mathbf{D}_{\text{SHELL}} = \begin{bmatrix} \frac{\partial_\alpha}{H_\alpha} & 0 & \frac{1}{H_\alpha R_\alpha} \\ 0 & \frac{\partial_\beta}{H_\beta} & \frac{1}{H_\beta R_\beta} \\ 0 & 0 & \partial_z \\ \partial_z - \frac{1}{H_\alpha R_\alpha} & 0 & \frac{\partial_\alpha}{H_\alpha} \\ 0 & \partial_z - \frac{1}{H_\beta R_\beta} & \frac{\partial_\beta}{H_\beta} \\ \frac{\partial_\beta}{H_\beta} & \frac{\partial_\alpha}{H_\alpha} & 0 \end{bmatrix} \tag{4.4}$$

where $\partial_x = \frac{\partial(\cdot)}{\partial_x}$, $\partial_y = \frac{\partial(\cdot)}{\partial_y}$, $\partial_\alpha = \frac{\partial(\cdot)}{\partial_\alpha}$, $\partial_\beta = \frac{\partial(\cdot)}{\partial_\beta}$, $\partial_z = \frac{\partial(\cdot)}{\partial_z}$, $H_\alpha = 1 + \frac{z}{R_\alpha}$, and $H_\alpha = 1 + \frac{z}{R_\beta}$.

Linear elastic isotropic materials are considered, leading to the following constitutive relation:

$$\boldsymbol{\sigma} = \mathbf{C}\boldsymbol{\epsilon} \tag{4.5}$$

C is the matrix of the material coefficients, see Bathe [60]. To derive the governing equations, the Principle of Virtual Displacements (PVD) is employed,

$$\delta L_{int} = \delta L_{ext} \tag{4.6}$$

Concerning the strain energy,

BEAM :

$$\delta L_{int} = \int_V \delta\boldsymbol{\epsilon}^T \boldsymbol{\sigma} dV = \int_V \left(\delta\epsilon_{xx}\sigma_{xx} + \delta\epsilon_{yy}\sigma_{yy} + \delta\epsilon_{zz}\sigma_{zz} + \delta\epsilon_{yz}\sigma_{yz} + \delta\epsilon_{xz}\sigma_{xz} + \delta\epsilon_{xy}\sigma_{xy}\right) dV \tag{4.7}$$

SHELL :

$$\delta L_{int} = \int_V \delta\boldsymbol{\epsilon}^T \boldsymbol{\sigma} dV = \int_V \left(\delta\epsilon_{\alpha\alpha}\sigma_{\alpha\alpha} + \delta\epsilon_{\beta\beta}\sigma_{\beta\beta} + \delta\epsilon_{zz}\sigma_{zz} + \delta\epsilon_{\beta z}\sigma_{\beta z} + \delta\epsilon_{\alpha z}\sigma_{\alpha z} + \delta\epsilon_{\alpha\beta}\sigma_{\alpha\beta}\right) dV \tag{4.8}$$

Through the displacement-strain relation, the CUF and the FEM approximations, and the constitutive equations, the fundamental nucleus of the stiffness matrix and load vector can be obtained [59]. For brevity, the remaining steps are omitted, and the explicit expression of the stiffness matrix nucleus is given in Appendix A. In the case of the plate/shell formulation, the Mixed Interpolation of the Tensorial Components (MITC) is used to alleviate locking [61].

5. ASYMPTOTIC-AXIOMATIC METHOD

The Asymptotic-Axiomatic Method (AAM) consists of using CUF to evaluate any structural theory's accuracy. The accuracy may be assessed on a single output, such as the maximum displacement, or an ensemble of outputs, e.g., the first ten natural frequencies. The reference solution may be various, e.g., an exact one - if available - or a high-fidelity numerical model. Figures 2a and 2b show a typical application of AAM. Four beam or shell theories are considered, each with various terms or DOF. CUF provides the governing equations and FEM matrices to run static or dynamic analyses, and the results from each theory are reported considering the error versus the reference solution. Such analysis can be repeated for an arbitrary number of theories and various sets of inputs, e.g., thickness ratios or boundary conditions. If all the combinations of terms up to a given order are considered, Figs. 2c and 2d can be obtained. A fourth-order shell theory (TE4) based on a Taylor expansion has, for example, 2^{15} reduced theories from combining the twelve terms of the expansion. The red line in Fig. 2d shows the shell theory providing the minimum error for a given number of terms.

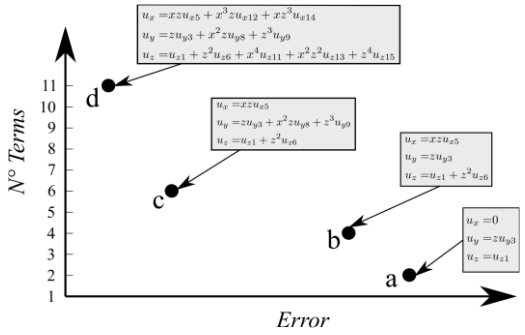

(a) Four beam theories

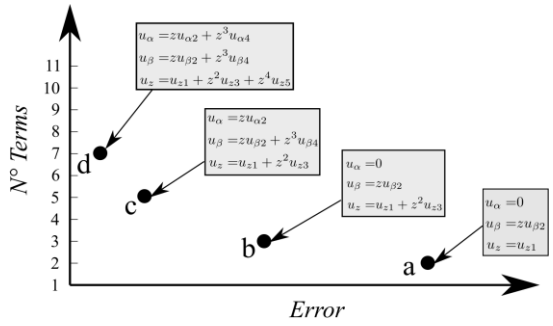

(a) Four shell theories

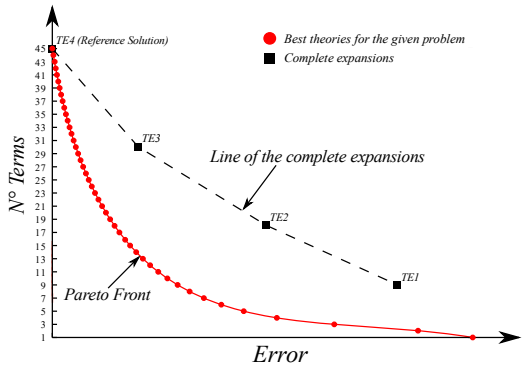

(c) Best Theory Diagram (BTD) for beam models

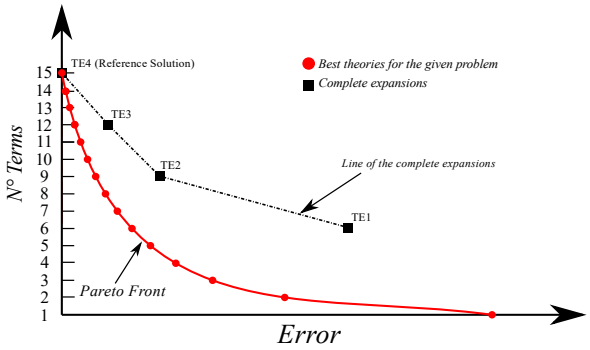

(d) Best Theory Diagram (BTD) for shell models

Fig. 2. Structural theories DOF and accuracy (a,b) and examples of Best Theory Diagrams (c,d)

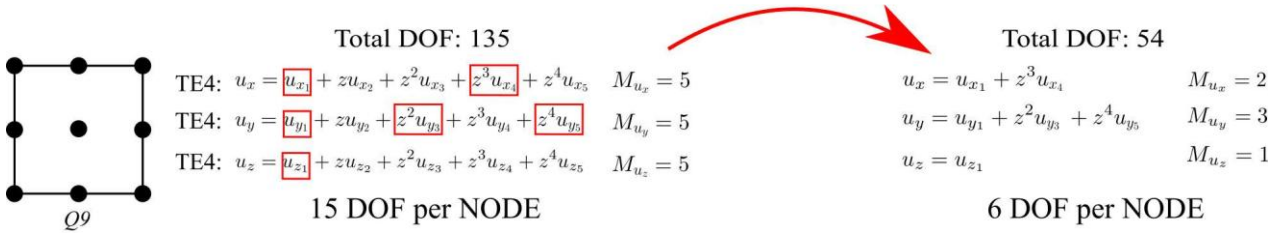

Fig. 3. Example of a full and reduced plate theory

Such a line may be seen as a Pareto front and is referred to as the Best Theory Diagram (BTD). For a given number of terms, it is impossible to have a better accuracy than a theory on the BTD. For a given accuracy level, obtaining it with fewer terms than a theory on the BTD is impossible. Once obtained, the BTD is useful to test any given theory's accuracy and computational efficiency. Figures 2c and 2d compare the complete expansion theories with the best models. In the result section, numerical cases are considered, and various theories are quantitatively compared. The present paper proposes a novel approach to implement the AAM. In previous works, reduced models were obtained through a penalization technique over the stiffness matrix. As a consequence, independently of the DOF of the reduced model, the full matrix had to be computed. The novel approach, instead, leads to the assembly of reduced matrices and, therefore, a reduced computational cost. As an example, a plate case is considered in the following. Let us consider the Q9 element in Fig. 3. A TE4 structural theory fourth-order Taylor uniform model is chosen as the reference solution, i.e., the Q9 element has 135 DOF and $M_{ux} = M_{uy} = M_{uz} = 5$. Then, a reduced model is considered with six DOF per node and 54 DOF per element, i.e., $M_{ux} = 2$, $M_{uy} = 3$ and $M_{uz} = 1$. Figure 4 shows the stiffness matrix and the load vector for the Q9 element. Each sub-matrix $\mathbf{K}_{ji}$, with, i,j = 1,...,9, has nine sub-matrices, and each sub-vector $\mathbf{P}_j$ consists of three sub-vectors. Circles highlight the terms related to i,j = 1. Figure 5 shows the circled sub-matrices and vectors. The grey rows and columns highlight the DOF included in the reduced model. The intersections between grey rows - the red squares - and columns are the matrix and vector components that must be computed. Figure 6 shows the i,j = 1 sub-matrix and vector for the reduced plate theory with six DOF per node. The global matrices and vectors can be assembled through standard FE assembly procedures. The related linear static analysis must be solved for each reduced model considered; e.g., if all reduced models stemming from the combination of twelve terms are considered, $2^{12} = 4096$ analyses are necessary.

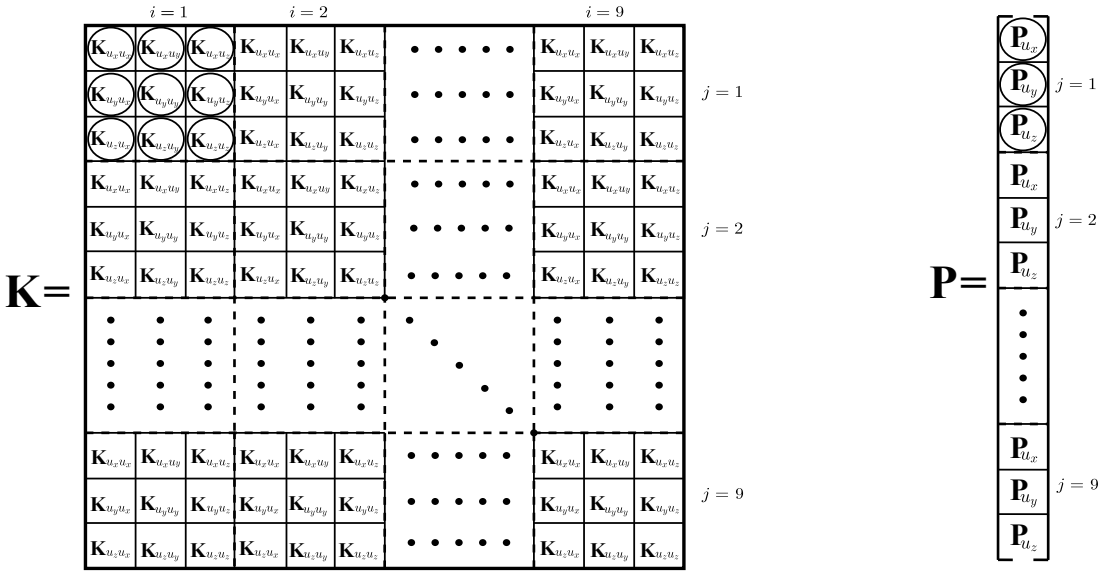

Fig. 4. Stiffness matrix and load vector of a Q9 element

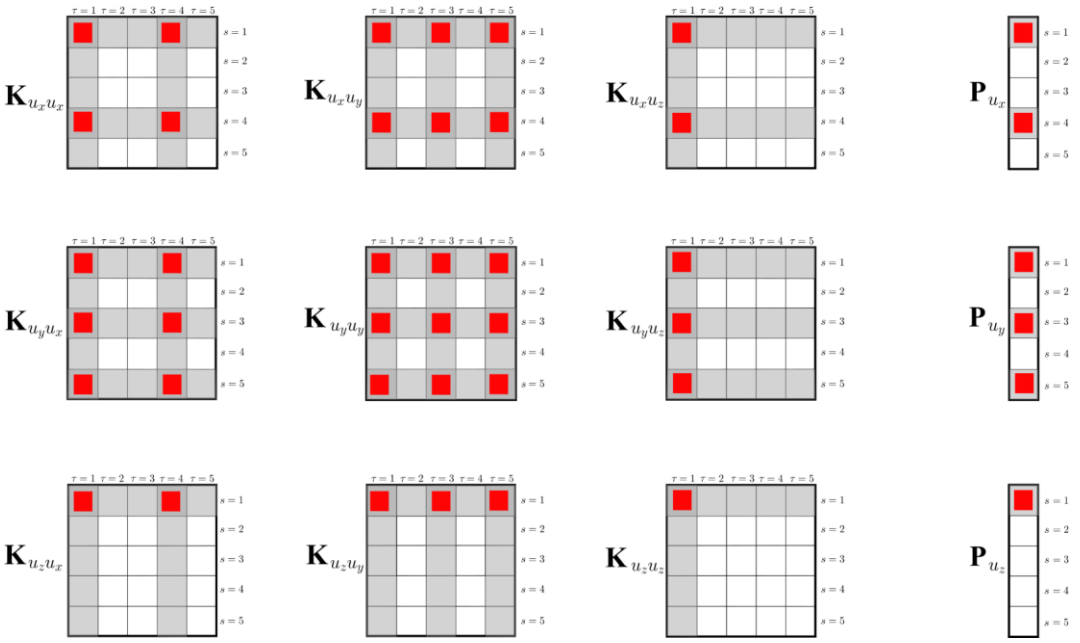

Fig. 5. Sub-matrices and vectors for i,j = 1

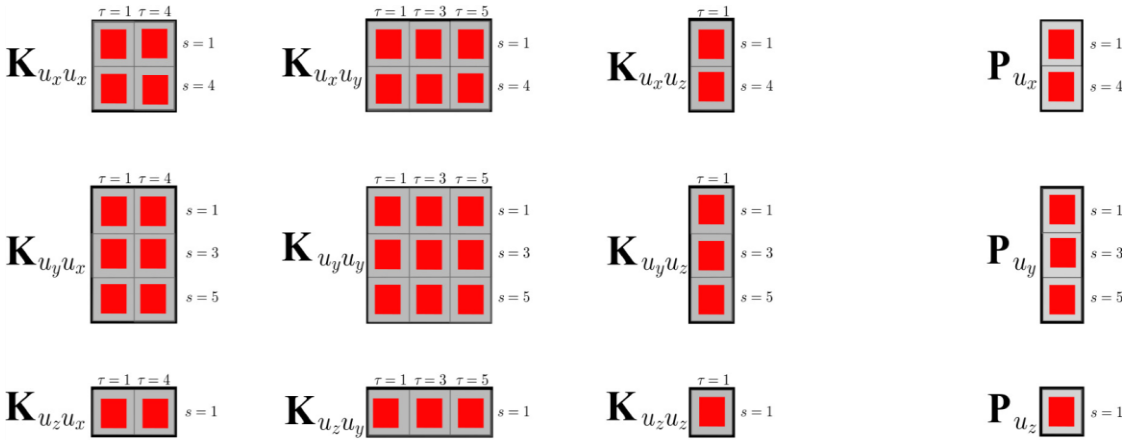

Fig. 6. Sub-matrices and vectors for i,j = 1 for the reduced plate model with six DOF per node

Table 1. TE4 beam theory

	1	x	z	x^2	xz	z^2	x^3	x^2z	xz^2	z^3	x^4	x^3z	x^2z^2	xz^3	z^4
u_x	•	•	•	•	•	•	•	•	•	•	•	•	•	•	•
u_y	•	•	•	•	•	•	•	•	•	•	•	•	•	•	•
u_z	•	•	•	•	•	•	•	•	•	•	•	•	•	•	•

Table 2. Example of a reduced beam theory with 11 DOF

	1	x	z	x^2	xz	z^2	x^3	x^2z	xz^2	z^3	x^4	x^3z	x^2z^2	xz^3	z^4
u_x	∘	∘	∘	∘	•	∘	•	∘	∘	∘	∘	∘	∘	•	∘
u_y	∘	∘	•	•	∘	∘	∘	∘	∘	•	∘	∘	∘	∘	∘
u_z	•	∘	∘	∘	∘	•	∘	∘	∘	∘	•	∘	•	∘	•

Complete and reduced theories can be conveniently shown in tabular form. Table (1) presents a complete TE4 beam theory with 45 DOF: black bullets indicate the generalized variables over the three displacement components. Table (2) shows a reduced beam theory where only eleven terms are included, with white circles indicating the inactive terms. Similarly, shell theories are shown in Tables (3) and (4).

6. NUMERICAL RESULTS

This section considers four cases: a beam with a compact cross-section, a clamped plate, a cylindrical shell under two pinching loads, and a shell under cylindrical bending. Concerning the shear locking, the selective reduced integration method is adopted for the beam formulation, while the MITC integration method is adopted for the plate/shell formulation.

Table 3. TE4 shell theory

	1	z	z^2	z^3	z^4
u_α	•	•	•	•	•
u_β	•	•	•	•	•
u_z	•	•	•	•	•

Table 4. Reduced shell theory with 10 DOF

	1	z	z^2	z^3	z^4
u_α	•	∘	•	∘	•
u_β	∘	∘	•	•	•
u_z	•	•	∘	•	•

6.1. Verification

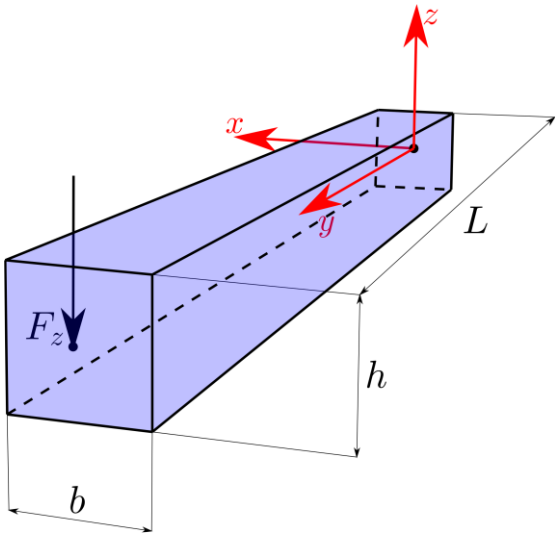

Fig. 7. Geometrical properties of the cantilever beam with compact cross-section [57].

The aim of this section is the verification of the results with a previous work of the authors [57]. The present paper builds BTD by assembling the FE matrices and arrays from the fundamental nucleus of each generalized variable. This section considers a cantilevered beam, previously analyzed in [57], see Fig. 7. The cross-section is clamped at y = 0, and the material properties are E = 75 (GPa) and $\nu = 0.33$. The height of the cross-section, h, is 0.2 (m), while the length, L, is 2 (m). The FE model consists of forty B4 elements, and a fourth-order Taylor expansion (TE4) is adopted over the cross-section as the reference solution complete model. The evaluation of reduced models uses the following error parameters:

$$\mathrm{err}_{u_z} = \left\| \frac{u_z^{TE4} - u_z}{u_z^{TE4}} \right\| \times 100 \quad \mathrm{err}_{u_y} = \left\| \frac{u_y^{TE4} - u_y}{u_y^{TE4}} \right\| \times 100 \tag{6.1}$$

$$\mathrm{err}_{\sigma_{yy}} = \left\| \frac{\sigma_{yy}^{TE4} - \sigma_{yy}}{\sigma_{yy}^{TE4}} \right\| \times 100 \tag{6.2}$$

Furthermore, consistently with [57], the following percentage variations are shown in Tables:

$$\delta_{u_z} = \frac{u_z}{u_z^{TE4}} \times 100 \quad \delta_{u_y} = \frac{u_y}{u_y^{TE4}} \times 100 \tag{6.3}$$

$$\delta_{\sigma_{yy}} = \frac{\sigma_{yy}}{\sigma_{yy}^{TE4}} \times 100 \tag{6.4}$$

The evaluation of the BTD should consider all 2^{45} combinations stemming from the forty-five generalized variables of a TE4. The reduction of the computational overhead was obtained by considering all three components of a given polynomial expansion simultaneously, e.g., all three

generalized displacements of the z^3 term were either active or off. Additionally, the three constant terms were always retained. Thus, the total combinations are 2^{14}=16384.

A point load, F_z=50 (N), is applied at [0,L,0], see Fig. 7. Figure 8 shows the BTD for the transverse displacement, u_z, computed at [0,L,0], i.e., the maximum transverse displacement. The vertical axis reports the number of active terms, i.e., the nodal degrees of freedom, of each structural theory evaluated. The horizontal axis reports the error of each theory; see Eq. 31. Each dot is a reduced structural theory combining the forty-five generalized displacement variables of the TE4. Models with the full linear (TE1), second- (TE2), third- (TE3), and fourth-order (TE4) expansions are reported for comparison purposes. Eventually, the BTD is given by the envelope of theories having the minimum error for a given number of terms. Similarly, Conversely, Figure 9 shows the BTD for σ_{yy} calculated at [0,0,h/2]. Tables 5 and 6 show the generalized displacement variables of the best theories composing the BTD. The first column reports the number of active terms. From the second column onwards, a black circle indicates that all three generalized displacements related to a given polynomial term are active; otherwise, the circle is white. The last column reports the error of the structural theory. For instance, the best theory with eighteen unknown variables has an error of 0.147%, and its displacement field is

$$\begin{aligned} u_x &= u_{x_1} + z u_{x_3} + x^2 u_{x_4} + xz u_{x_5} + z^2 u_{x_6} + z^3 u_{x_{10}} \\ u_y &= u_{y_1} + z u_{y_3} + x^2 u_{y_4} + xz u_{y_5} + z^2 u_{y_6} + z^3 u_{y_{10}} \\ u_z &= u_{z_1} + z u_{z_3} + x^2 u_{z_4} + xz u_{x_5} + z^2 u_{z_6} + z^3 u_{z_{10}} \end{aligned} \tag{6.5}$$

Table 5. Square cross-section beam, bending load, best theories for u_z

N Terms	1	x	z	x^2	xz	z^2	x^3	x^2z	xz^2	z^3	x^4	x^3z	x^2z^2	xz^3	z^4	err[%]
45	•	•	•	•	•	•	•	•	•	•	•	•	•	•	•	0.00
42	•	◦	•	•	•	•	•	•	•	•	•	•	•	•	•	0.00
39	•	◦	•	•	•	•	•	•	◦	•	•	•	•	•	•	0.00
36	•	◦	•	•	•	•	◦	•	◦	•	•	•	•	•	•	0.00
33	•	◦	•	•	•	•	◦	•	◦	•	•	•	•	◦	•	0.00
30	•	◦	•	•	•	•	◦	•	◦	•	•	•	◦	◦	•	0.011
27	•	◦	•	•	•	•	◦	•	◦	•	◦	•	◦	◦	•	0.027
24	•	◦	•	•	•	•	◦	◦	◦	•	◦	•	◦	◦	•	0.069
21	•	◦	•	•	•	•	◦	◦	◦	•	◦	◦	◦	◦	•	0.101
18	•	◦	•	•	•	•	◦	◦	◦	•	◦	◦	◦	◦	◦	0.147
15	•	◦	•	•	•	•	◦	◦	◦	◦	◦	◦	◦	◦	◦	0.265
12	•	◦	•	◦	•	•	◦	◦	◦	◦	◦	◦	◦	◦	◦	3.01
9	•	◦	•	◦	◦	•	◦	◦	◦	◦	◦	◦	◦	◦	◦	10.63
6	•	◦	•	◦	◦	◦	◦	◦	◦	◦	◦	◦	◦	◦	◦	31.79
3	•	◦	◦	◦	◦	◦	◦	◦	◦	◦	◦	◦	◦	◦	◦	99.33

The verification of the results considers the comparisons of the accuracy of the following structural theories, retrieved from [57]:

$$\text{Model 1b:}\quad \begin{aligned} u_x(x,y,z) &= 0 \\ u_y(x,y,z) &= zu_{y_3} \\ u_z(x,y,z) &= u_{z_1} \end{aligned} \tag{6.6}$$

$$\text{Model 2b:}\quad \begin{aligned} u_x(x,y,z) &= xzu_{x5} \\ u_y(x,y,z) &= zu_{y_3} \\ u_z(x,y,z) &= u_{z_1} + z^2u_{z6} \end{aligned} \tag{6.7}$$

$$\text{Model 3b:}\quad \begin{aligned} u_x(x,y,z) &= xzu_{x5} \\ u_y(x,y,z) &= zu_{y_3} + x^2zu_{y8} + z^3u_{y10} \\ u_z(x,y,z) &= u_{z_1} + z^2u_{z6} \end{aligned} \tag{6.8}$$

$$\text{Model 4b:}\quad \begin{aligned} u_x(x,y,z) &= xzu_{x5} + x^3zu_{x12} + xz^3u_{x14} \\ u_y(x,y,z) &= zu_{y_3} + x^2zu_{y8} + z^3u_{y10} \\ u_z(x,y,z) &= u_{z_1} + z^2u_{z6} + x^4u_{z11} + x^2z^2u_{z13} + z^4u_{z15} \end{aligned} \tag{6.9}$$

Table 6. Square cross-section beam, bending load, best theories for σ_{yy}

N Terms	1	x	z	x^2	xz	z^2	x^3	x^2z	xz^2	z^3	x^4	x^3z	x^2z^2	xz^3	z^4	err[%]
45	•	•	•	•	•	•	•	•	•	•	•	•	•	•	•	0.00
42	•	◦	•	•	•	•	•	•	•	•	•	•	•	•	•	0.00
39	•	◦	•	•	•	•	•	•	◦	•	•	•	•	•	•	0.00
36	•	◦	•	•	•	•	◦	•	◦	•	•	•	•	•	•	0.00
33	•	◦	•	•	•	◦	◦	•	◦	•	•	•	•	•	•	0.015
30	•	◦	•	•	•	◦	◦	◦	◦	•	•	•	•	•	•	0.015
27	•	◦	•	•	•	◦	◦	◦	◦	•	◦	•	•	•	•	0.047
24	•	◦	•	•	◦	◦	◦	◦	◦	•	◦	•	•	•	•	0.027
21	•	◦	•	◦	◦	◦	◦	◦	◦	•	◦	•	•	•	•	0.027
18	•	◦	•	◦	◦	◦	◦	◦	◦	•	◦	•	•	•	◦	0.027
15	•	◦	•	◦	◦	◦	◦	◦	◦	•	◦	•	•	◦	◦	0.027
12	•	◦	•	◦	◦	◦	◦	◦	◦	•	◦	◦	•	◦	◦	1.25
9	•	◦	•	◦	◦	◦	◦	◦	◦	•	◦	◦	◦	◦	◦	9.32
6	•	◦	•	◦	◦	◦	◦	◦	◦	◦	◦	◦	◦	◦	◦	12.69
3	•	◦	◦	◦	◦	◦	◦	◦	◦	◦	◦	◦	◦	◦	◦	100

Table 7 shows the accuracy parameter for the transverse displacement and axial stress; δ_{uz}, for instance, is 100 % when a perfect match of transverse displacements with the reference solution is found. All first-order models have the Poisson locking correction activated. The first column reports the structural theories considered, while the second column has the number of variables of a theory for the three displacement components. For instance, the ”2b” has one variable for u_x and u_y and two

for u_z. The third and fourth columns show the accuracy, and the last column shows each model's total degrees of freedom.

Table 7. Square cross-section beam, bending load, verification of accuracy of selected theories

Model	M_{u_x} /M_{u_y} /M_{u_z}	$\delta^a_{u_z}$[%]	$\delta^b_{\sigma_{yy}}$[%]	DOF
First-order				
TE1[57]	3/3/3	100.7	87.3	1089
Model 1b[57]	0/1/1	100.7	87.3	242
Model 1b	0/1/1	100.7	87.3	242
Second-order				
TE2[57]	6/6/6	99.7	89.6	2178
Model 2b[57]	1/1/2	96.7	89.6	484
Model 2b	1/1/2	96.7	89.6	484
Third-order				
TE3[57]	10/10/10	99.9	97.5	3630
Model 3b[57]	1/3/2	97.1	98.5	726
Model 3b	1/3/2	97.1	98.5	726
Fourth-order				
TE4[57]	15/15/15	100	100	5445
Model 4b[57]	3/3/5	99.5	100	1331
Model 4b	3/3/5	99.5	100	1331

(a): Computed at [0,L,0]; (b): Computed at [0,0,h/2]

Figures 8 and 9 show the Best Theory Diagrams (BTD) obtained by considering u_z and σ_{yy}, respectively. The horizontal axis is the error of a given structural theory; the vertical axis reports each theory's number of terms or nodal degrees of freedom. Every dot is a structural theory obtained by combining the generalized variables of a fourth-order beam theory. The solid line is the BTD, i.e., the set of theories that provides the minimum error for a given number of unknown variables. For the sake of comparison, lower-order theories are reported as well. The results suggest the following:

- There is a perfect match between the reference results and the present ones, i.e., the new approach to building reduced models, based on the manipulation of the FE matrices, is equivalent to the penalization technique adopted in previous works.
- As well-known, linear terms are crucial for bending beams. Second- and third-order ones are not negligible due to the moderate slenderness of the beam considered.

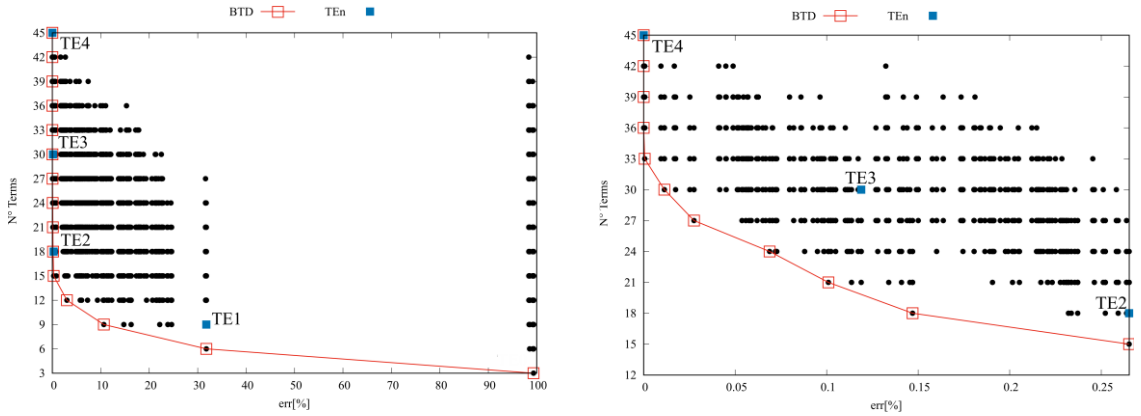

(a) Complete plot (b) Zoomed plot

Fig. 8. Square cross-section beam, bending load, BTD for u_z

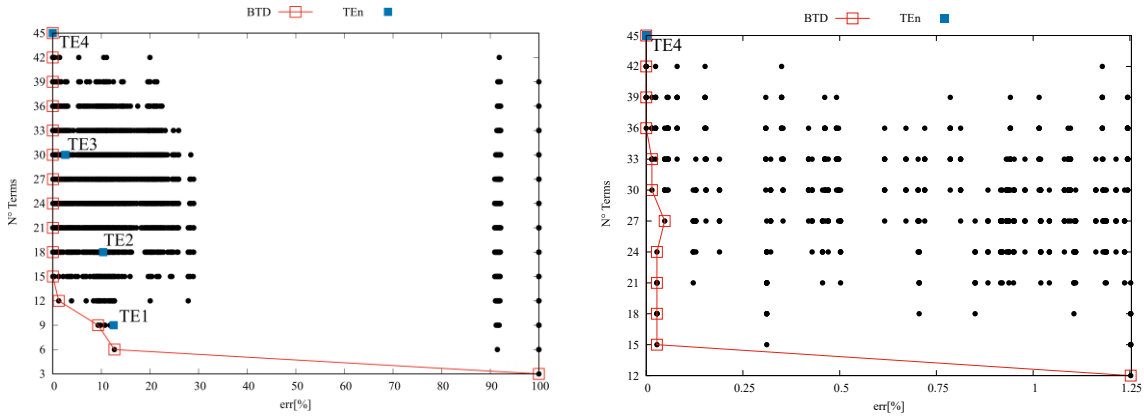

(a) Complete plot (b) Zoomed plot

Fig. 9. Square cross-section beam, bending load, BTD for σ_{yy}

6.2. End-Effects

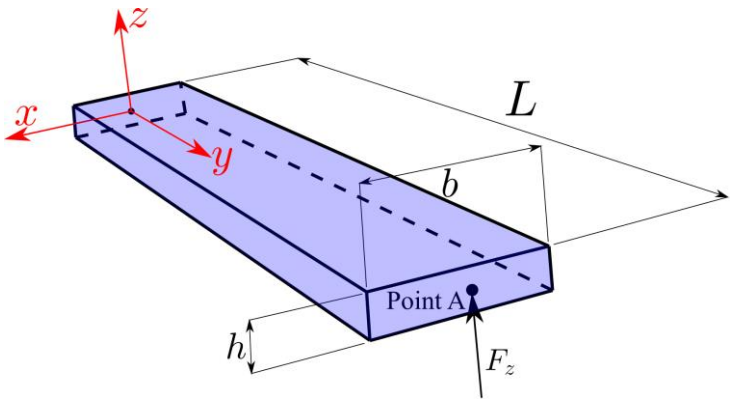

Fig. 10. Cantilever structure with a point load [62, 63]

The second case concerns the end-effects in a cantilever structure. Ghazouani and El Fatmi [62] initially proposed this analysis, and it was further investigated by Carrera *et al.* [63]. Figure 10 shows the geometrical properties of the structure; L/h = 6 and b/h = 0.5. The material has the following properties: $E_{11} = 206.80$ (GPa), $E_{22} = E_{33} = 5.17$ (GPa), $G_{12} = G_{13} = 3.10$ (GPa), $G_{23} = 2.55$ (GPa), and $\nu_{12} = \nu_{23} = \nu_{23} = 0.25$. The plate is clamped at y=0, and a 1 (N) force is applied at [0, L, 0].

The axial stress, σ_{yy}, is evaluated along y, at x = 0 and z = h/2. The results are compared with a higher-order beam theory (1D-SV) [62], a 3D FEM solution (3D-FEM) [62], and a 1D CUF-based solution (1D-TE5) [63], which utilizes a fifth-order Taylor expansion. For all the analyses, ninety MITC9 finite elements are adopted.

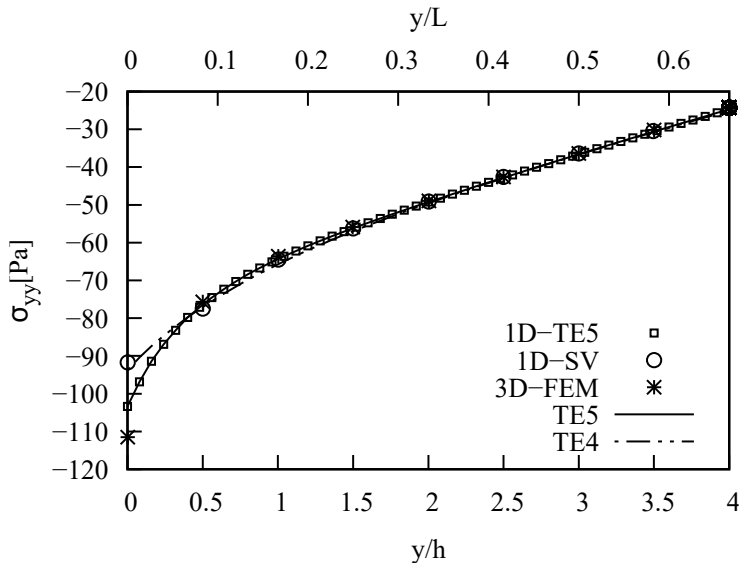

Fig. 11. σ_{yy} along the axis from various models

Figure 11 compares the literature solutions with the present TE5 plate model. Given the perfect match with solutions from the literature, TE5 is chosen as the reference solution to build the BTD, i.e.,

$$\mathrm{err}_{\sigma_{yy}} = \left\| \frac{\sigma_{yy}^{TE5} - \sigma_{yy}}{\sigma_{yy}^{TE5}} \right\| \times 100 \tag{6.10}$$

σ_{yy} is taken at [0,0,h/2]. Figure 12 shows the BTD. The constant terms of the three displacement variables are kept active in each model to limit the number of combinations. Four best theories are explicitly reported on Fig. 13.

Table 8 compares the accuracy of various models concerning σ_{yy}, evaluated at [0,0,h/2]. Full expansions and best models, as shown in Fig. 13, are reported. Figure 14 shows the stress distribution along the axis from the reference solutions and the best theories.

The results suggest that:

- As well-known, end-effects are relevant only near the clamped region.
- The proper detection of the end-effects requires higher-order terms. The axial displacement's third- and fifth-order terms, z^3u_{y4} and z^5u_{y6}, are necessary to have errors lower than 5%.
- Best models with satisfactory accuracy require significantly less DOF than the reference solution. Six terms are enough to detect the axial stress near the clamped region.

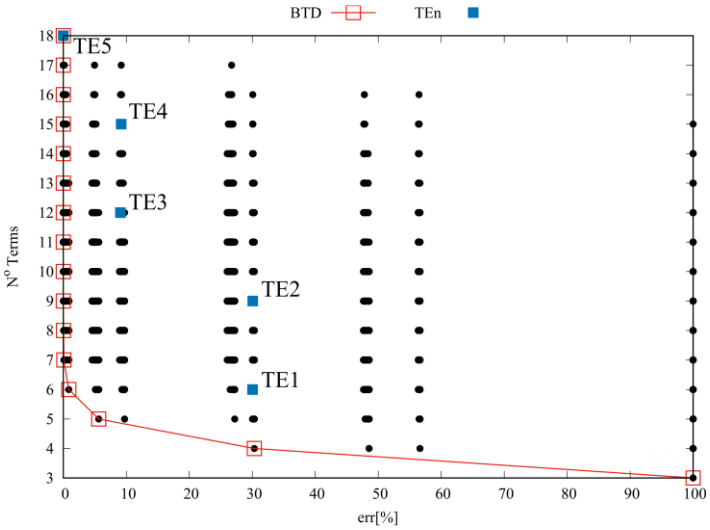

Fig. 12. Cantilever structure, BTD for σ_{yy}

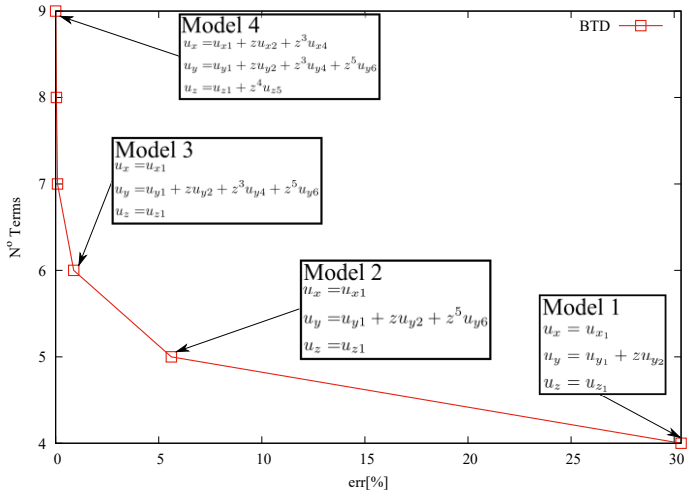

Fig. 13. Cantilever structure, four best theories for σ_{yy}

Table 8. Cantilever structure, σ_{yy}, at [0,0,h/2] from various models

Model	$M_{u_x}/M_{u_y}/M_{u_z}$	$-\sigma_{yy}[Pa]$	err[%]	DOF
Full expansion models				
TE1	2/2/2	72.239	30.106	2730
TE2	3/3/3	72.256	30.088	4095
TE3	4/4/4	93.976	9.0734	5460
TE3	5/5/5	93.848	9.1979	6825
TE4	6/6/6	103.35	—[a]	8190
Best models from Fig. 13				
Model 1	1/2/1	72.000	30.336	1820
Model 2	1/3/1	97.554	5.6114	2275
Model 3	1/4/1	102.45	0.8787	2730
Model 4	3/4/2	103.33	0.0186	4095

(a): Reference solution

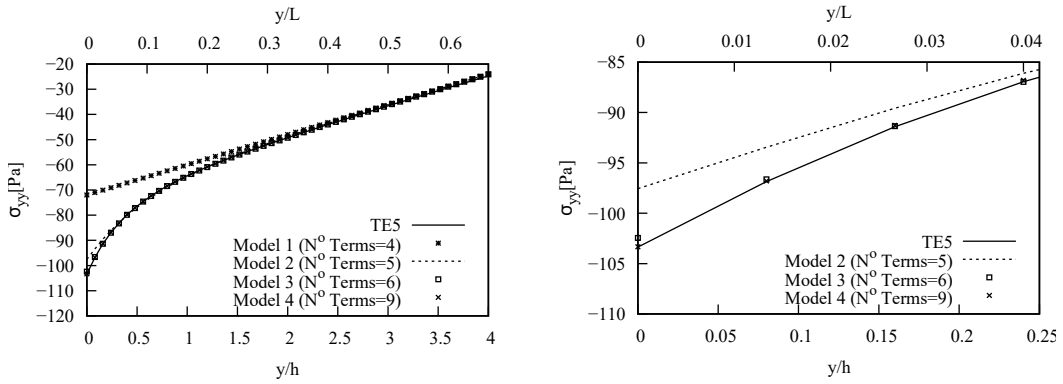

(a) Complete plot (b) Zoomed plot

Fig. 14. Cantilever structure, σ_{yy} along y, at x=0 and z=h/2, from various models

6.3. Pinching loads

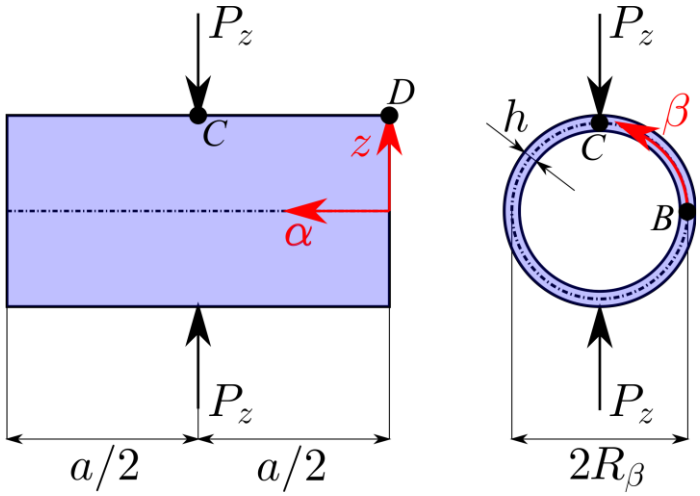

Fig. 15. Geometrical properties and loading conditions of the cylindrical shell under two pinching loads [64]

A thin-walled cylindrical shell is considered; see Fig. 15. The geometrical data are $a/R_\beta = 2$, $R_\beta/h = 100$, and $b = 2\pi R_\beta$. An isotropic material is considered, and its properties are $E = 3\times10^6$ (psi) and $\nu = 0.3$. The cylinder is simply supported at $\alpha = 0$ and $\alpha = a$. Two pinching concentrated forces, P_z, are applied at [a/2, ± b/4, h/2] and are equal to 10^4 (lb). This benchmark was taken from the classical work of Lindberg *et al.* [64] with the solution obtained through the Fluegge equations [65]. The results consider the transverse displacement, u_z, and the dimensionless form is

$$\bar{u}_z = \frac{Eh}{P_z} u_z \tag{6.11}$$

Due to the symmetry of the structure and loading conditions, one-eighth of the cylinder was considered and discretized using a uniform 13×13 mesh. Although a convergence analysis was performed, its details are omitted here for brevity.

Figure 16 shows the dimensionless transverse displacement along two lines, BC [a/2,β,0] and DC [α,b/4,0], respectively. The results from the literature are compared with complete expansion theories. Since the results from TE3 and TE4 are identical, TE3 is set as the reference solution to build the BTD. Figure 17 shows the BTD based on the transversedisplacement at [a/2,b/4,0] and the following error:

$$\text{err} = \left\| \frac{\bar{u}_z^{TE3} - \bar{u}_z}{\bar{u}_z^{TE3}} \right\| \times 100 \tag{6.12}$$

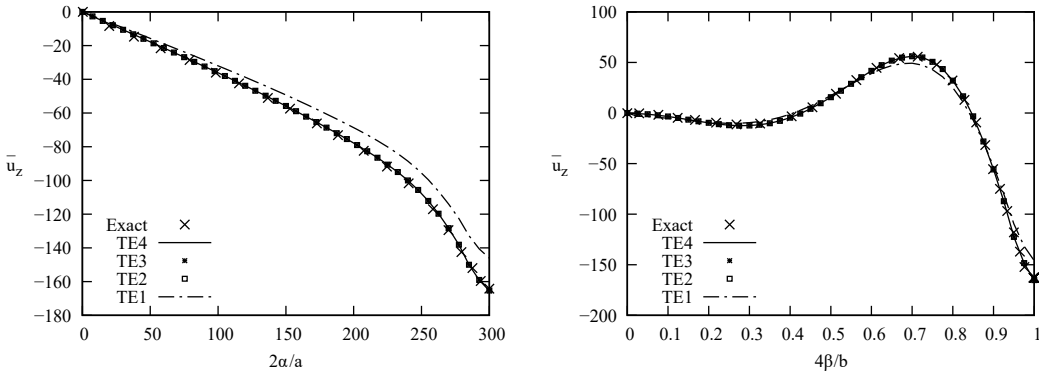

(a) Along DC [α,b/4,0] (b) Along BC [a/2,β,0]

Fig. 16. Shell under two pinching loads, $\bar{u}_z$ from various models

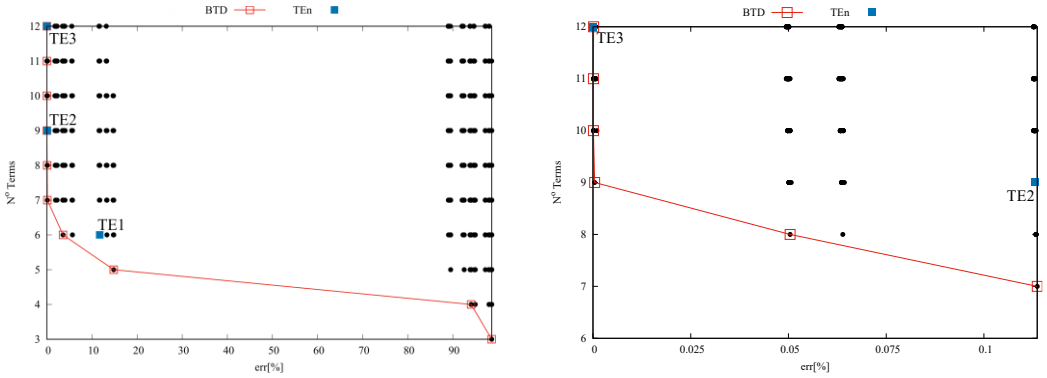

(a) Complete plot (b) Zoomed plot

Fig. 17. Shell under two pinching loads, BTD

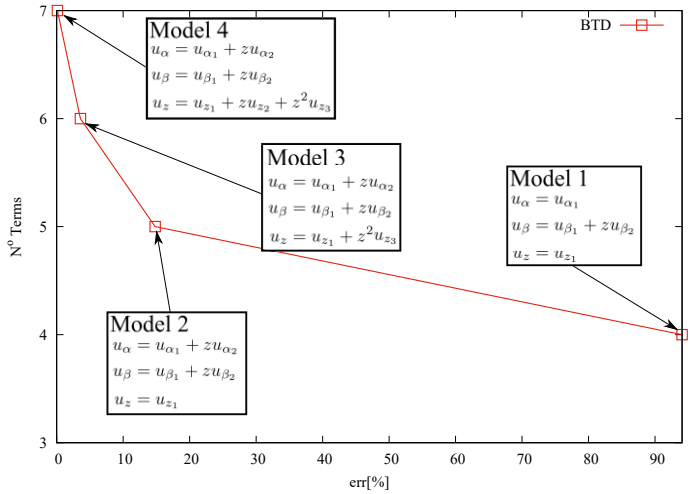

Fig. 18. Shell under two pinching loads, four best models for $\bar{u}_z$

The constant terms of the three displacement variables are always active in each model, as in the previous cases. Figure 18 shows the explicit expressions of four best models, and Table 9 compares the results of the four best models with the full expansion ones. Figure 19 shows the transverse displacements obtained through the best models.

Table 9. Shell under two pinching loads, $\bar{u}_z$, at [a/2,b/4,0] from various models

Model	$M_{u_x}/M_{u_y}/M_{u_z}$	$\bar{u}_z$	err[%]	DOF
Full expansion models				
TE1$^{(Corr)}$	2/2/2	-176.45	6.645	4374
TE1$^{(No\ Corr)}$	2/2/2	-146.09	11.703	4374
TE2	3/3/3	-165.27	0.114	6561
TE3	4/4/4	-165.45	—[a]	8748
Best models from Fig. 18				
Model 1	1/2/1	-9.8173	94.1	2916
Model 2	2/2/1	-140.94	14.8	3645
Model 3	2/2/2	-159.61	3.53	4374
Model 4	2/2/3	-165.27	0.114	5103

(a): Reference solution

The analysis of the results suggests that

- Overall, there is a good match with the exact solution in most cases.
- The inclusion of normal stretching is crucial to obtain acceptable accuracy.
- The linear and parabolic terms of the transverse displacement are necessary to have errors lower than 4%, while linear terms along the other two directions are enough.

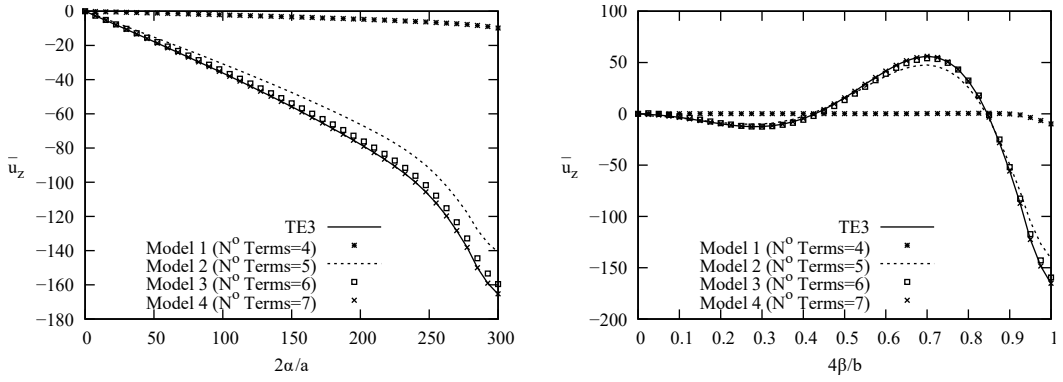

(a) Along DC [α,b/4,0] (b) Along BC [a/2,β,0]

Fig. 19. Shell under two pinching loads, u_z from best theories

6.4. Cylindrical bending

The last numerical case considers the shell shown in Fig. 20, and previously presented by Carrera *et al.* [66], where the penalization technique was adopted. Here, the new method has been

employed. The structure is a thick shell with a radius-to-thickness ratio of R_β/h =4 and a = 1 (m). The shell is simply-supported along the edges in the α-direction and has a sinusoidal pressure p = $p_z \sin\left(\frac{\pi\beta}{b}\right)$, with p_z = 1 (Pa). The material properties are E = 73 (GPa) and ν = 0.34. The transverse displacement, evaluated at [a/2,b/2,z], is adimensionalized as follows:

$$\bar{u}_z = \frac{10Eu_z h^3}{p_z R_\beta^4} \tag{6.13}$$

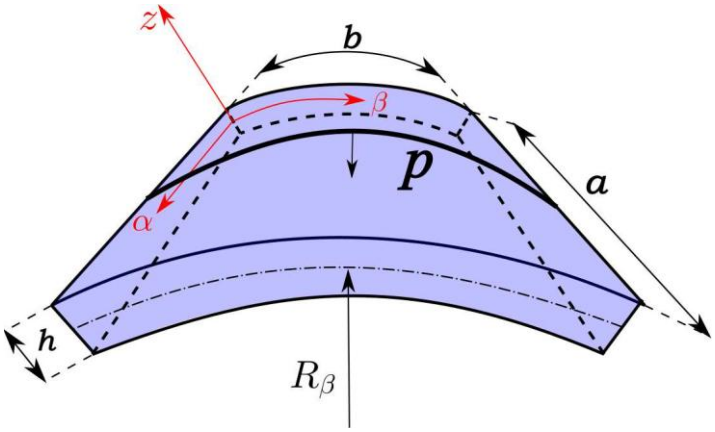

Fig. 20. Geometrical properties and loading conditions of shell under sinusoidal pressure [66]

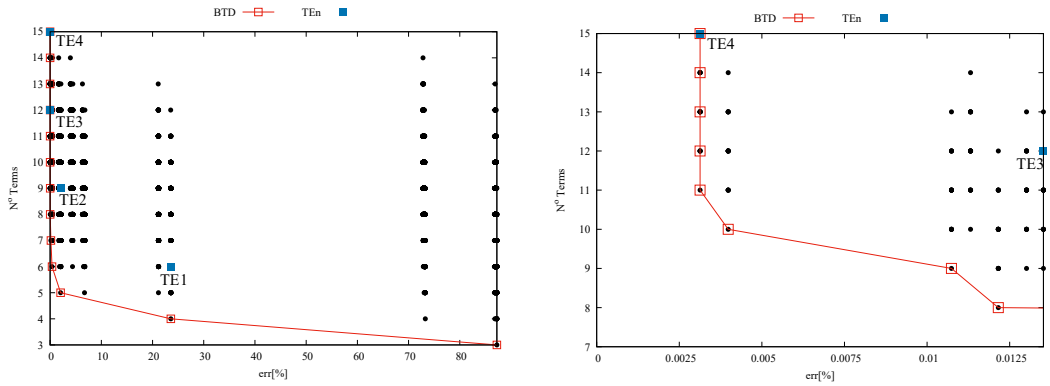

(a) Complete plot (b) Zoomed plot

Fig. 21. Cylindrical bending of a shell, BTD

The results are compared with a Navier-type closed-form solution with a Legendre-based fourth-order structural theory [45]. The following analyses adopt ten MITC9 finite elements along the β-axis and one along the α-axis. Figure 21 shows the BTD the best theory diagram and the error is:

$$\text{err} = \left\| \frac{\bar{u}_z^{LD4} - \bar{u}_z}{\bar{u}_z^{LD4}} \right\| \times 100 \tag{6.14}$$

Figure 22 shows the explicit expressions of four best theories. Table 10 shows the results from various models, including the best theories from Fig. 22.

The results suggest the following:

- The influence of higher-order terms is less relevant than in the previous cases.

- Second-order terms along the thickness and third-order along the other directions are crucial to improve the solution.

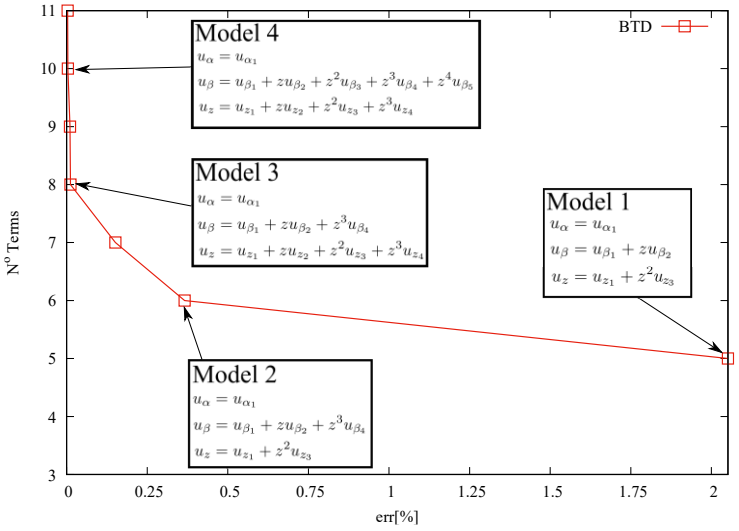

Fig. 22. Cylindrical bending of a shell, four best theories for $\bar{u}_z$

Table 10. Cylindrical bending of a shell, $\bar{u}_z$, at [a/2,b/2,0] from various models

Model	$M_{u_x}/M_{u_y}/M_{u_z}$	$\bar{u}_z$	err[%]	DOF
	Literature [66]			
LD4	5/5/5	2.1213	—[a]	—[b]
	Uniform models			
TE1(Corr)	2/2/2	1.6208	0.476	378
TE1(No Corr)	2/2/2	2.1112	23.59	378
TE2	3/3/3	2.0763	2.119	567
TE3	4/4/4	2.1210	0.014	756
TE4	5/5/5	2.1214	0.003	945
	Reduced models			
Model 1	1/2/2	2.0778	2.055	315
Model 2	1/3/2	2.1135	0.366	378
Model 3	1/3/4	2.1210	0.012	504
Model 4	1/5/4	2.1214	0.003	630

(a): Reference solution; (b): N/A

7. CONCLUSIONS

This paper has presented numerical results concerning the selection of generalized variables for beam, plate, and shell theories. The approach adopted is based on the Carrera Unified Formulation and allows for the development of higher-order expansions, which may differ for each displacement component and may consider arbitrary terms, i.e., it is not restricted to full expansions of a given order and can skip terms. The proper manipulation of finite element matrices leads to the systematic evaluation of the accuracy of structural theories stemming from any combinations of generalized

variables. The theories providing the best accuracy with the minimum number of variables are referred to as ”best” and are presented through Best Theory Diagrams. The numerical results concern structural problems with significant localized effects, e.g., pinched shells or end-effect problems. The following conclusions may be drawn:

- As well known, properly choosing generalized variables is highly problem-dependent.
- In all cases considered, the variables having a decisive role are much less than those of full expansions, i.e., their proper selection can lead to significant reductions in the computational cost.
- Third-order terms are often necessary for acceptable accuracy. Similarly, through-thethickness stretching is necessary in most cases.

Future research efforts should explore applying the present approach to more complex structures and nonlinear and multifield analyses. Furthermore, the possibility to vary the kinematics node-wise will be investigated.

REFERENCES

1. L. Euler, *Methodus inveniendi lineas curvas maximi minimive proprietate gaudentes sive solutio problematis isoperimetrici latissimo sensu accepti*, Volume 1: (Springer Science & Business Media, Berlin, Germany, 1952).
2. S. P. Timoshenko, “On the transverse vibrations of bars of uniform cross section,” Philos. Mag. **43**, 125–131 (1922). doi: https://doi.org/10.1080/14786442208633855.
3. R. K. Kapania and S. Raciti, “Recent advances in analysis of laminated beams and plates. Part I: Shear effects and buckling,” AIAA J. **27**:923–935 (1989). doi: https://doi.org/10.2514/3.10202.
4. R. K. Kapania and S. Raciti, “Recent advances in analysis of laminated beams and plates. Part II: Vibrations and wave propagation,” AIAA J. **27**, 935–946 (1989). doi: https://doi.org/10.2514/3.59909.
5. K. Washizu. *Variational Methods in Elasticity and Plasticity*. (Pergamon, Oxford, United Kingdom, 1968).
6. V. Z. Vlasov. *Thin-walled elastic beams*. (National Technical Information Service, Washington DC, USA, 1984).
7. P. O. Friberg, “Beam element matrices derived from Vlasov’s theory of open thin-walled elastic beams,” Int. J. Numer. Methods Eng. **21**, 1205–1228 (1985). doi: https://doi.org/10.1002/nme.1620210704.
8. I. Mechab, N. El Meiche, and F. Bernard, “Analytical study for the development of a new warping function for high order beam theory,” Compos. B: Eng. **119**, 18–31 (2017). doi: https://doi.org/10.1016/j.compositesb.2017.03.006.

9. R. Schardt, “Eine Erweiterung der Technischen Biegetheorie zur Berechnung prismatischer Faltwerke,” STAHLBAU **35**, 161–171 (1966).
10. M. Ganapathi, B. P. Patel, O. Polit, and M. Touratier, “A C^1 finite element including transverse shear and torsion warping for rectangular sandwich beams,” Int. J. Numer. Methods Eng. **45**, 47–75 (1999). doi: https://doi.org/10.1002/nme.1082.
11. M. Levinson, “A new rectangular beam theory,” J. Sound Vibration **74**, 81–87 (1981). doi: https://doi.org/10.1016/0022-460X(81)90493-4.
12. X. Wang and S. Li. “Free vibration analysis of functionally graded material beams based on Levinson beam theory,” Appl. Math. Mech. **37**, 861–878 (2016). doi: https://doi.org/10.1007/s10483-016-2094-9.
13. T. Kant and B. S. Manjunath, “Refined theories for composite and sandwich beams with C finite elements,” Comput. Struct. **33**, 755–764 (2014). doi: https://doi.org/10.1016/0045-7949(89)90249-6.
14. T. Kant and B. S. Manjunatha, “Higher-order theories for symmetric and unsymmetric fiber reinforced composite beams with C finite elements,” Finite Elem. Anal. Des. **6**, 303–320 (1990). doi: https://doi.org/10.1016/0168-874X(90)90022-7.
15. B. S. Manjunatha and T. Kant, “Different Numerical Techniques for the Estimation of Multiaxial Stresses in Symmetric/Unsymmetric Composite and Sandwich Beams with Refined Theories,” J. Reinf. Plast. Compos. **12**, 2–37, (1993). doi: https://doi.org/10.1177/073168449301200101.
16. R. Kapania and V. Goyal, “Free vibration of uncertain unsymmetrically laminated beams,” *19th AIAA Applied Aerodynamics Conference*, **1**, 1–11 (2001). doi: https://doi.org/10.2514/6.2001-1317.
17. X.-B. Bui, T.-K. Nguyen, N.-D.Nguyen, and T. P. Vo, “A general higher-order shear deformation theory for buckling and free vibration analysis of laminated thin-walled composite I-beams,” Compos. Struct. 295, 115775 (2022). doi: https://doi.org/10.1016/j.compstruct.2022.115775.
18. E. Carrera and G. Giunta., “Refined beam theories based on a unified formulation,” Int. J. Appl. Mech. **2**, 117–143 (2010). doi: https://doi.org/10.1142/S1758825110000500.
19. E. Carrera, G. Giunta, P. Nali, and M. Petrolo, “Refined beam elements with arbitrary cross section geometries,” Comput. Struct. **88**, 283–293 (2010). doi: https://doi.org/10.1016/j.compstruc.2009.11.002.
20. E. Carrera and M. Petrolo, “Refined beam elements with only displacement variables and plate/shell capabilities,” Meccanica **47**, 537–556 (2012). doi: https://doi.org/10.1007/s11012-011-9466-5.

21. P. M. Naghdi, “A survey of recent progress in the theory of elastic shells,” Appl. Mech. Rev. **9**, 365–368 (1956).
22. G. Kirchhoff, “Uber das Gleichgewicht und die Bewegung einer elastischen Scheibe,” J. fur Reine Angew. Math. **40**, 51–88 (1850).
23. E. Reissner, “The effect of transverse shear deformation on the bending of elastic plates” J. App. Mech. Trans. ASME **12**, 69–77 (1945). doi: https://doi.org/10.1115/1.4009435.
24. R. D. Mindlin, “Influence of rotary inertia and shear on flexural motions of isotropic, elastic plates,” J. App. Mech. Trans. ASME **18**, 31–38 (1951). doi: https://doi.org/10.1115/1.4010217.
25. J. N. Reddy, *Mechanics of laminated composite plates and shells: theory and analysis*, (CRC Press, New York, USA, 1997).
26. J. N. Reddy and D. H. Robbins, “Theories and Computational Models for Composite Laminates,” Appl. Mech. Rev. **47**, 147–169 (1994). doi: https://doi.org/10.1115/1.3111076.
27. A. K. Noor and W. S. Burton, “Assessment of computational models for multilayered composite shells,” Appl. Mech. Rev. **43**, 67–97 (1990). doi: https://doi.org/10.1115/1.3119162.
28. B. D Annin and Y. M. Volchkov, “Nonclassical models of the theory of plates and shells,” J. Appl. Mech. Tech. Phy., **57**, 769–776 (2016). doi: https://doi.org/10.1134/S0021894416050011.
29. E. Carrera, I. Elishakoff, and M. Petrolo, “Who needs refined structural theories?,” Compos. Struct. **264**,113671 (2021). doi: https://doi.org/10.1016/j.compstruct.2021.113671.
30. Q. Fan, Y. Zhang, L. Dong, S. Li, and S. N. Atluri, “Are higher-order theories and layer-wise zig-zag theories necessary for N-layer composite laminates?,” CMES Comput. Model. Eng. Sci. **107**, 155–186 (2015). doi: https://doi.org/10.3970/cmes.2015.107.155.
31. E. I. Grigolyuk and F. A. Kogan, “State of the art of the theory of multilayer shells,” Sov. Appl. Mech. **8**, 583–595 (1972). doi: https://doi.org/10.1007/BF00892606.
32. E. I. Grigolyuk and G. M. Kulikov, “General direction of development of the theory of multilayered shells,” Mech. Compos. Mater. **24**, 231–241 (1988). doi: https://doi.org/10.1007/BF00608158.
33. T. Kant, D. R. J. Owen, and O.C. Zienkiewicz, “A refined higher-order C plate bending element,” Comput. Struct. 15, 177–183 (1982). doi: https://doi.org/10.1016/00457949(82)90065-7.
34. T. Kant and B. S. Manjunatha, “An unsymmetric FRC laminate C finite element model with 12 degrees of freedom per node,” Eng. Comput. **5**, 300–308 (1988). doi: https://doi.org/10.1108/eb023749.
35. B. N. Pandya and T. Kant, “Finite element analysis of laminated composite plates using a higher-order displacement model,” Compos. Sci. Technol. **32**, 137–155 (1988). doi: https://doi.org/10.1016/0266-3538(88)90003-6.

36. M. P. Sheremetev and B. L. Pelekh, “Construction of refined plate theory,” *Eng. Mag.*, **4**, 34–41 (1964). (in Russian).
37. J. M. Whitney and N. J. Pagano, “Shear Deformation in Heterogeneous Anisotropic Plates,” J. Appl. Mech. Trans. ASME **37**, 1031–1036 (1970). doi: https://doi.org/10.1115/1.3408654.
38. J. N. Reddy, “A simple higher-order theory for laminated composite plates,” J. Appl. Mech. Trans. ASME **51**,745–752 (1984). doi: https://doi.org/10.1115/1.3167719.
39. J. N. Reddy and C. F. Liu, “A higher-order shear deformation theory of laminated elastic shells,” Int. J. Eng. Sci. **23**, 319–330 (1985). doi: https://doi.org/10.1016/0020-7225(85)90051-5.
40. J. Awrejcewicz, V. A. Krysko, M. V. Zhigalov, I. V. Papkova, and V. A. Krysko, “Mathematical models for quantifying flexible multilayer orthotropic shells under transverse shear stresses,” Compos. Struct. **204**, 896–911 (2018). doi: https://doi.org/10.1016/j.compstruct.2018.07.052.
41. A. Bhimaraddi, “A higher order theory for free vibration analysis of circular cylindrical shells,” Int. J. Solids Struct. **20**, 623–630 (1984). doi: https://doi.org/10.1016/0020-7683(84)90019-2.
42. F. B. Hildebrand, E. Reissner, and G. B. Thomas, “Notes on the Foundations of the Theory of Small Displacement of Orthotropic Shells,” NACA TN-1833, (1940).
43. R. K. Khare, T. Kant, and A. K. Garg, “Free vibration of composite and sandwich laminates with a higher-order facet shell element,” Compos. Struct. **65**, 405–418 (2004). doi: https://doi.org/10.1016/j.compstruct.2003.12.003.
44. E. Carrera, “Multilayered shell theories accounting for layerwise mixed description, Part 2: Numerical evaluations,” AIAA J. **37**, 1117–1124 (1999). doi: https://doi.org/10.2514/2.822.
45. E. Carrera, “Theories and Finite Elements for Multilayered Plates and Shells: A Unified compact formulation with numerical assessment and benchmarking,” Arch. Comput. Methods Eng. **10**, 215–296 (2003). doi: https://doi.org/10.1007/BF02736224.
46. A. Pagani, E. Carrera, D. Scano, and R. Augello, “Finite elements based on Jacobi shape functions for the analysis of beams, plates and shells,” Int. J. Numer. Methods Eng. **124**, 4490–4519 (2023). doi: https://doi.org/10.1002/nme.7316.
47. D. Scano, E. Carrera, and M. Petrolo, “Use of the 3D Equilibrium Equations in the Free-Edge Analyses for Laminated Structures with the Variable Kinematics Approach,” Aerotec. Missili Spaz. **103**, 179–195 (2024). doi: https://doi.org/10.1007/s42496-02300177-2.
48. V. V. Volovoi, D. H. Hodges, V. L. Berdichevsky, and V. G. Sutyrin, “Asymptotic theory for static behavior of elastic anisotropic I-beams,” Int. J. Solids Struct. **36**, 1017–1043 (1999). doi: https://doi.org/10.1016/S0020-7683(97)00341-7.
49. V. V. Volovoi and D. H. Hodges, “Theory of Anisotropic Thin-Walled Beams,” J. Appl. Mech. Trans. ASME **67**, 453–459 (2000). doi: https://doi.org/10.1016/09619526(92)90035-5.

50. B. Popescu and D. H. Hodges, “On asymptotically correct Timoshenko-like anisotropic beam theory,” Int. J. Solids Struct. **37**, 535–558 (2000). doi: https://doi.org/10.1016/S0020-7683(99)00020-7.
51. W. Yu, D. H. Hodges, V. Volovoi, and C. E.S. Cesnik, “On Timoshenko-like modeling of initially curved and twisted composite beams,” Int. J. Solids Struct. **39**, 5101–5121 (2002). doi: https://doi.org/10.1016/S0020-7683(02)003992.
52. A. L. Gol’denveizer, *Theory of Elastic Thin Shells*, (Pergamon Press, Oxford, UK, 1961).
53. P. Cicala, Sulla teoria elastica della parete sottile, Giornale del Genio Civile, fascicoli 4, 6 e 9, 1959.
54. P. Cicala, *Systematic Approximation Approach to Linear Shell Theory*, (Levrotto e Bella, Turin, Italy, 1965).
55. C.-Y. Lee and D. H. Hodges, “Asymptotic construction of a dynamic shell theory: Finite-element-based approach,” Thin-Walled Struct. **47**, 256–270 (2009). doi: https://doi.org/10.1016/j.tws.2008.08.004.
56. V. L. Berdichevsky, “An asymptotic theory of sandwich plates,” Int. J. Eng. Sci. **48**, 383–404 (2010). doi: https://doi.org/10.1016/j.ijengsci.2009.09.001.
57. E. Carrera and M. Petrolo, “On the Effectiveness of Higher-Order Terms in Refined Beam Theories,” J. Appl. Mech. Trans. ASME **78**, (2010). doi: https://doi.org/10.1115/1.4002207.
58. M. Petrolo and P. Iannotti, “Best Theory Diagrams for Laminated Composite Shells Based on Failure Indexes,” Aerotec. Missili Spaz. **102**, 199–218 (2023). doi: https://doi.org/10.1007/s42496-023-00158-5.
59. E. Carrera, M. Cinefra, M. Petrolo, and E. Zappino. *Finite element analysis of structures through unified formulation*. (Wiley, Chichester, UK, 2014).
60. K. J. Bathe, *Finite Element Procedure*, (Prentice Hall, Upper Saddle River, USA, 1996).
61. M. L. Bucalem and K. J. Bathe, “Higher-order MITC general shell elements,” Int. J. Numer. Methods Eng. **36**, 3729–3754 (1993). doi: https://doi.org/10.1002/nme.1620362109.
62. N. Ghazouani and R. El Fatmi, “Higher order composite beam theory built on Saint-Venant’s solution. Part II: Built-in effects influence on the behavior of end-loaded cantilever beams,” Compos. Struct. **93**, 567–581 (2011). doi: https://doi.org/10.1016/j.compstruct.2010.08.023.
63. E. Carrera, M.Petrolo, and E. Zappino, “Performance of CUF approach to analyze the structural behavior of slender bodies,” J. Struct. Eng. **138**, 285–297 (2012). doi: https://doi.org/10.1061/(ASCE)ST.1943-541X.0000402.

64. G. M. Lindberg, M. D. Olson, and G. R. Cowper. “New Developments in the Finite Element Analysis of Shells,” Quarterly Bulletin of the Division of Mechanical Engineering and The National Aeronautical Establishment **4**, 1–38 (1969).
65. W. Fluegge, *Statik und Dynamic der Schalen*, (Springer-Verlag, Berlin, Germany, 1934).
66. E. Carrera, M. Cinefra, A. Lamberti, and M. Petrolo, “Results on best theories for metallic and laminated shells including layer-wise models,” Compos. Struct. **126**, 285–298, (2015). doi: https://doi.org/10.1016/j.compstruct.2015.02.027.

A. FUNDAMENTAL NUCLEI FOR BEAMS, PLATES, AND SHELLS

1D beam:

$$K_{u_x u_x s\tau ji} = C_{11}\int_L N_j N_i dy \int_A F_{u_x s,x} F_{u_x \tau,x} dxdz + C_{55}\int_L N_j N_i dy \int_A F_{u_x s,z} F_{u_x \tau,z} dxdz + C_{66}\int_L N_{j,y} N_{i,y} dy \int_A F_{u_x s} F_{u_x \tau} dxdz \tag{A.1}$$

2D shell:

$$\begin{aligned} K_{u_\alpha u_\alpha s\tau ji} &= C_{11} N_{j,\alpha}^{n1} N_{i,\alpha}^{m1} \int_\Omega N_{n1} N_{m1} d\alpha d\beta \int_A F_{u_\alpha s} F_{u_\alpha \tau} \frac{H_\beta}{H_\alpha} dz \\ &+ C_{55} N_j^{n1} N_i^{m1} \int_\Omega N_{n1} N_{m1} d\alpha d\beta \int_A F_{u_\alpha s,z} F_{u_\alpha \tau,z} H_\alpha H_\beta dz \\ &- C_{55} \frac{1}{R_\alpha} N_j^{n1} N_i^{m1} \int_\Omega N_{n1} N_{m1} d\alpha d\beta \int_A F_{u_\alpha s,z} F_{u_\alpha \tau} H_\beta dz \\ &- C_{55} \frac{1}{R_\alpha} N_j^{n1} N_i^{m1} \int_\Omega N_{n1} N_{m1} d\alpha d\beta \int_A F_{u_\alpha s} F_{u_\alpha \tau,z} H_\beta dz \\ &+ C_{55} \frac{1}{R_\alpha^2} N_j^{n1} N_i^{m1} \int_\Omega N_{n1} N_{m1} d\alpha d\beta \int_A F_{u_\alpha s} F_{u_\alpha \tau} \frac{H_\beta}{H_\alpha} dz \\ &+ C_{66} N_{j,\beta}^{n3} N_{i,\beta}^{m3} \int_\Omega N_{n3} N_{m3} d\alpha d\beta \int_A F_{u_\alpha s} F_{u_\alpha \tau} \frac{H_\alpha}{H_\beta} dz \end{aligned} \tag{A.2}$$

2D Plate may be seen as a particular case of the shell formulation,

$$\begin{aligned} K_{u_x u_x s\tau ji} &= C_{11} N_{j,x}^{n1} N_{i,x}^{m1} \int_\Omega N_{n1} N_{m1} dxdy \int_A F_{u_x s} F_{u_x \tau} dz \\ &+ C_{55} N_j^{n1} N_i^{m1} \int_\Omega N_{n1} N_{m1} dxdy \int_A F_{u_x s,z} F_{u_x \tau,z} dz \\ &+ C_{66} N_{j,y}^{n3} N_{i,y}^{m3} \int_\Omega N_{n3} N_{m3} dxdy \int_A F_{u_x s} F_{u_x \tau} dz \end{aligned} \tag{A.3}$$